SM Online
Scientific Resources

SM Journal of Hematology and Oncology

Research Article

High Throughput siRNA Screen Identifies LRP8 as Druggable Metabolic Regulator in Triple-Negative Breast Cancer

Banu Arun[1], Soley Bayraktar[1], Christine Shiang[4], Yuan Qi[2], Bailiang Wang[1], Angelica GB[1], Fraser SW[3], Liem Phan[5], Mong-Hong Lee[5], Yun Wu[3], Gabriel NH[1], Vikram W[6] and Lajos P[6]*

[1]*Departments of Breast Medical Oncology, University of Texas, M.D. Anderson Cancer Center, USA*
[2]*Departments of Biostatistics, University of Texas, M.D. Anderson Cancer Center, USA*
[3]*Departments of Pathology, University of Texas, M.D. Anderson Cancer Center, USA*
[4]*Program in Experimental Therapeutics, University of Texas Graduate School of Biomedical Sciences, USA*
[5]*Molecular and Cellular Oncology, Okayama University, Japan*
[6]*Yale Cancer Center, Yale School of Medicine, USA*

Article Information

Received date: Sep 17, 2016
Accepted date: Nov 11, 2016
Published date: Nov 30, 2016

***Corresponding author**

Lajos Pusztai, Yale Cancer Center, Yale School of Medicine, 333 Cedar St, PO Box 208032 New Haven, USA, Email: lajos.pusztai@yale.edu

Abstract

Background: Triple-Negative Breast Cancers (TNBC) overexpress a large number of genes compared to other breast cancer subtypes and these genes represent potential therapeutic targets.

Methods: We identified genes overexpressed in TNBC compared in public gene expression data sets and performed an siRNA screen with 4 distinct constructs against each of 681 overexpressed genes in 18 breast cancer cell lines. The top tier hits were assessed in functional and mechanistic studies to validate their role in the growth and survival of TNBC cells *in vitro* and *in vivo*.

Results: Low density Lipoprotein Receptor-Related Protein 8 (LRP8) and Very Low-Density Lipoprotein Receptor (VLDLR) was the top two ranked hits based on 3 of 4 siRNAs showing, significant and preferential growth inhibition in TNBC cell lines. Apolipoprotein E isoform 4 (ApoE4), and to a lesser extent rellin, which are ligands of both LRP8 and VLDLR stimulated the growth of TNBC cells *in vitro* in a receptor-dependent manner. Suppression of LRP8 or VLDLR expression or exposure to a ligand inhibitor, RAP abolished this ligand-induced proliferation. Metabolic profiling (with GC/MS and LC/MSMS) and reverse phase protein arrays (n=230 antibodies/201 proteins) revealed that ApoE4 stimulation rescued TNBC cells from serum-starvation, induced up-regulation of genes involved in lipid biosynthesis and increased protein expression of genes involved in the MAPK/ERK and DNA repair pathways.

Conclusion: LRP8 is overexpressed in TNBC and promotes cell growth and survival under nutrient depleted conditions through stimulating lipid biosynthetic pathways. Inhibitors of LRP8/VLDLR signaling represent potential new therapeutic targets for TNBC.

Translational Relevance

We identified 681 genes that were consistently and significantly overexpressed in TNBC in multiple data sets and performed a siRNA screen including each of these genes on 18 breast cancer cell lines. Two closely related cell surface receptors, LRP8 and VLDLR showed the most consistent inhibitory effect in our siRNA screen. Both of these receptors mediate cholesterol and lipid trafficking through binding to apoliporotein E (ApoE) in peripheral tissues and function as stress signaling pathways through binding reelin in neural cells in the central nervous system. Down regulation of either LRP8 or VLDLR, or blocking of ApoE binding to these receptors, results in increased apoptosis *in vitro* and *in vivo*. The relatively low expression of LRP8 in most normal tissues coupled with its high expression in TNBC and its essential function for cell survival under nutrient stress renders it a potential novel therapeutic target for this disease.

Introduction

Triple-Negative Breast Cancers (TNBC) is defined as tumors that lack expression of Estrogen Receptor (ER), Progesterone Receptor (PR), and express Human Epidermal Growth Factor Receptor-2 (HER2) at normal levels [1]. TNBC affects 10-17% of all invasive breast cancers and is associated with poor prognosis [2,3]. The lack of a well-characterized target for treatment leaves only systemic chemotherapy as the mainstay of treatment. Targeted therapies that take advantage of the unique molecular perturbations found in TNBC are needed.

Results from high-throughput microarray analyses revealed large-scale gene expression, DNA copy number and mutation distribution differences between TNBC and other subtypes of breast

cancers [4-9]. However, there are no recurrent, high frequency mutations or copy number abnormalities in TNBC other than mutations in p53, and less commonly PI3K mutations. [10-12]. On the other hand, there are a large number of genes that are consistently overexpressed in TNBC relative to other breast cancer subtypes [5,8,9]. We hypothesize that some of these overexpressed genes may represent novel, breast cancer subtype-specific therapeutic targets [13]. The purpose of the current project was to assess the functional importance of genes overexpressed in TNBC and discover novel therapeutic targets for TNBC.

Materials and Methods

Identification of genes overexpressed in TNBC

The discovery sets included 2 independent breast cancer gene expression data sets (GSE16716 (n=294), GSE2034 (n=286) [16,17]. Receptor status was determined through mRNA expression values of ER and HER2 as described previously [18]. Unequal variance t-test was used to identify differentially expressed genes and false discovery rates (FDR) were calculated using the method by Ponds et al. [19]. The union of differentially overexpressed genes were tested in 2 additional datasets, GSE7390 and GSE11121, to define the final gene list that was consistently overexpressed in all 4 data sets [20,21]. Cell line gene expression data were obtained from Array Express accession number E-TABM-157 (n=51) and from Liedtke et al. (n=19, cell line data set from M.D. Anderson Cancer Center) to test if the genes overexpressed in TNBC tissue from patients also overexpressed in TNBC cell lines [22,23]. All cell lines were obtained from the American Type Culture Collection (ATCC) for the purpose of these experiments and no further authentication was performed. Cell line certificates are available at: https://www.atcc.org/Products/Collections/Cell_Biology_Collections/Cell_Lines/Human/Alphanumeric/HTB-26.aspx#documentation.

siRNA screen

The siRNA screen included 681 genes in 10 TNBC, 8 non-TNBC cell lines using 4 independent siRNA constructs purchased from Dharmacon (Supplementary Table 1). The siRNA screen was performed in 384-well plates at 37^0C for 96 hours. Cells were seeded at a density that yields about 70-90% confluence in the control wells at 96 hours. The final concentration of all siRNA constructs was 40nM per well in 50μl total volume in 3 parallel replicates. A control plate, including only replicates of positive and negative siRNA controls and cells grown in OptiMEM media alone, was inserted after every 10 test plates to assess assay stability. The optimum transfection condition was defined as the experimental setting that maximized the Z-factor, computed as Z=1-(3 x SSD/R) where R is the dynamic range of the assay (i.e. the absolute difference between mean cell viability for a given negative control and positive control), and SSD is the sum of the standard deviations for the positive and negative control assays (Supplementary Table 2). Cell viability was determined by the Cell Titer Blue assay (Promega, Madison, WI) using a Beckman Coulter Biomek 3000 reader 96 hours after transfection. Cell viability was calculated as follows; median value of absorbance in wells containing media alone was subtracted from absorbance readings of all other wells, individual readings of each test wells was divided by the median value of absorbance corresponding to negative siRNA control wells in the same plate and the fraction was multiplied by 100 to derive percent viability. Average percent viability across the 3 replicate plates was reported for each siRNA construct. Unequal variance t-test was used to assess significant decrease in viability compared to control wells.

Plasmid rescue experiments for LRP8 and VLDLR

To test the specificity of siRNA results, two distinct silent mutations were introduced into the siRNA binding regions of LRP8 or VLDLR (LRP8 NM_001018054, CTGGACTGACTCGGGCAATAA to CTGGACTGACTCAGGTAATAA, CTCAACGGTGTGGACCGGCAA to CTCAACGGCGTAGACCGGCAA, VLDLR NM_001018056, CAAGATCGTAGGATAGTACTA to CAAGATCGTAGAATAGTACTA, CAAGGTTGGTAGACATGTTAA to CAAGGTTGGTAGGCACGTTAA, Sigma Aldrich) to create rescue plasmids. Cells were transfected with siLRP8 or siVLDLR alone or in combination with the siRNA resistant rescue plasmid. Cells were treated with the rescue plasmid for 48 hours followed by treatment with the respective siRNA for another 48 to 72 hours. Cell viability was assessed at 48 and 72 hours after siRNA transfection using the CellTiter 96_ AQueous One Solution Cell Proliferation Assay (Promega).

To assess mRNA down regulation, total RNA was extracted using the Qiagen RNeasy kit and reverse transcribed into cDNA and quantitative real-time PCR were performed with primers Hs00171168_m1 and Hs01045922_m1 (Applied Biosystems) for LRP8 and VLDLR, respectively. To determine LRP8 and VLDLR protein levels, cell lysates were collected in RIPA buffer, total protein was quantitated using the BCA Protein Assay (ThermoFisher Scientific, Pittsburgh, PA) and western blotting was performed using antibodies (H00007804-M01 from Novus, at dilution 1:500 and NB110-68193 also from Novus, at dilution 1:1000, respectively.

Ligand stimulation studies

Reelin and the Apolipoprotein E (ApoE) isoforms 2, 3, and 4 were obtained from R&D Systems and MBL International and were dissolved in deionized, distilled water. Cells were treated with 0.030, 0.060, or 0.120 nM reelin and 150, 300, 600 or 1200 nM of ApoE isoforms for 72 hours. TNBC cells were grown in serum-free media to study the effects of ApoE. Low density lipoprotein receptor-related protein associated protein 1 (RAP1, Enzo Life Sciences), a nonspecific inhibitor of LRP8 ligand binding, was added at 200nM in combination with the ApoE isoforms to determine ligand-dependent effects. Cell growth was assessed at 24, 48, and 72 hours. Independent experiments were performed three times for each cell line.

BrdU incorporation and apoptosis assays

Cells were treated with 25 nM siLRP8 or siVLDLR and exposed to 600 or 1200 nM ApoE4. Bromodeoxyuridine incorporation was measured at 48 and 72 hours using the BrdU Cell Proliferation ELISA assay (Roche Applied Science, Indianapolis, IN). Caspase-3/7 activity was assayed at 48 and 72 hours after treatment using the Apo-ONE Homogeneous Caspase-3/7 Assay (Promega, Madison, WI).

ApoE4/LRP8 solid-phase ELISA assay

Recombinant human LRP8-Histidine tagged (R&D Systems, catalog number 3520-AR) was bound overnight to nickel coated 96 well black plates (ThermoFisher Scientific, catalog number 15342) at a final concentration of 10^5pM at 4^0C. ApoE4 conjugated to horseradish peroxidase (ApoE4-HRP, Novus, catalog number NBP1-49529H, 1:2000) was incubated with the LRP8 coated wells for 1 hour

at room temperature followed by two 0.01% PBS with Tween-20. In this assay, we tested the effects of RAP and 3 distinct commercially available anti-LRP8 antibodies including LRP8 mouse monoclonal antibody targeting amino acids 83-171 (Novus, catalog number H00007804-M01), ApoER2/LRP8 polyclonal antibody targeting the C-terminus (Novus, catalog number NBP1-96573), and mouse IgG as an isotype control (Abcam, catalog number ab37355). RAP was tested at concentrations ranging from 0.01 to 1000 nM and the antibodies were used at final concentrations of 0.01 to 1000 ug/mL. Ligand binding was quantified using Thermo Scientific QuantaBlu Fluorogenic Peroxidase Substrate Kits (catalog number 15162) at excitation 315-340 nm and emission 370-470 nm.

Gene expression, proteomic, and metabolic effects of LRP8 activation by ApoE4

To assess the effects of ApoE4 stimulation on RNA and protein expression and on the phosphorylation status of important regulatory proteins, RNA and protein were isolated from control (grown in serum free media) and ApoE4 treated (600nM) BT-549 and MDA-MB-436 cells at baseline (0h) and at 8 and 48 hours. Gene expression profiling was performed using Affymetrix U133A gene chips and protein analysis was done using a reverse phase protein array with 230 antibodies against 201 proteins [13,14,25]. All gene expression and proteomic profiling experiments were performed in triplicates. Unequal variance t-test was used to identify differentially expressed genes and FDR was calculated as described above. Ingenuity Pathway Analysis tools were used to map genes to pathways. To assess metabolic changes induced by ApoE4, BT-549 parental cells as well as siLRP8 and si-Control cells were exposed to 600 nM ApoE4 in serum-free medium or were grown either in regular media or serum-free media as controls. After 48 hours, cells were harvested with trypsinization, washed in PBS, and were stored in liquid nitrogen, until shipment to Metabolon, Inc (Durham, NC) for metabolic profiling. Metabolomic profiling was performed in six replicates using Gas Chromatography/Mass Spectrometry (GC/MS) and liquid chromatography/tandem mass spectrometry (LC/MSMS) as described previously [26].

shLRP8 MDA-MB-231 stable knockdown cell line

To generate stable knockdown of LRP8 in MDA-MB-231 cells we used lentiviral shRNA purchased from (Sigma-Aldrich, St. Louis, MO, clones TRCN0000055498 and TRCN0000055499). Target cells were transduced with each shLRP8 clone at an MOI of 20 and polybrene (Sigma-Aldrich, St. Louis, MO) at a final concentration of 8μg/mL. 48 hours after transduction, cells were selected with 4μg/mL puromycin (Sigma-Aldrich, St. Louis, MO) in DMEM-F12 media (Invitrogen, Grand Island, NY) and were maintained in DMEM-F12 media with 2μg/mL puromycin. Stable knockdown clones were selected using GFP expression and LRP8 protein levels were assessed with Western blotting.

shLRP8 MDA-MB-231 mouse xenograft studies

Female Athymic Nude-Foxn1 Nude Mice (Nu/Nu) were purchased from Harlan (Indianapolis, Indiana USA) and used when they were 8 weeks old. For all *in vivo* experiments, MDA-MB-231 tumor cells stably transfected with shRNA against LRP8 and harvested in the exponential growth phase by brief exposure to a 0.25% trypsin/0.02% EDTA. The cells were washed, re-suspended in PBS and cell viability was assessed using trypan blue exclusion. Single-cell suspensions of >95% viability were diluted to 2 x 10^6 tumor cells in 0.1mL of RPMI-1640 serum free medium with 50% Matrigel (BD Matrigel, BD Biosciences, San Jose, CA, USA) and were injected subcutaneously at the 4th pair mammary glands. Tumor growth was monitored by palpation and the onset of tumors was noted. Tumor size was measured with digital calipers and tumor volume was calculated assuming an ellipsoid shape with the following equation: Tumor volume (mm^3) = (Length x $Width^2$) x π/6. The animals were killed 10 weeks after tumor cell inoculation. Afterwards, subcutaneous tumors were harvested and weighed. Individual tumors were split for fixation in 4% paraformaldehyde for histology and immunostaining and flash frozen in liquid nitrogen for RNA and protein collection. Organs were fixed in Bouin's solution for 24 hours to differentiate neoplastic lesions from organ parenchyma. Metastases were counted with the aid of a dissecting microscope, and confirmed by routine histology. Representative data were obtained from five mice per experimental group.

Immunohistochemistry

Fifty-nine formalin fixed paraffin embedded breast cancer samples (ER-negative n=23, ER-positive n=25) were assessed with immunohistochemistry for LRP8 expression. Slides were rehydrated with deionized and distilled water; antigen retrieval was performed with citrate buffer. Slides were exposed to 3% hydrogen peroxide x 15 minutes, washed in TBS, blocked with avidin and biotin and rinsed in TBS. All slides were blocked for 15 minutes with whole serum from the animal species corresponding to the secondary antibody. LRP8 (Abnova PAB4740 -rabbit polyclonal antibody) was diluted at 1:50 and VLDLR (Abcam ab 62543 - mouse monoclonal antibody) was diluted at 1:50 with TBS buffer and applied to sections for one hour at room temperature. The association between clinicopathologic variables (age, ER and HER2 status, stage, nuclear grade, Ki67 expression) and LRP8 protein expression was tested. P-values were based on Fisher's exact test with N≤5 (two-sided, 95% confidence interval, $\alpha<0.05$). LRP8 protein expression was divided into ordinal variables as strong, moderate, or weak expression, or dichotomized as LRP8 positive (>1% cells show staining) versus negative.

Results

Target identification in gene expression data and siRNA screen

In the first discovery dataset (GSE16716), 1871 probe sets were overexpressed in TNBC compared to non-TNBC (FDR<0.00001). 62% of these (n=1162) were also overexpressed ($p<0.05$) in TNBC in the validation set (GSE2034). We next removed probe sets with <2.0 fold overexpression and with p-values >0.0001 in the validation data and tested overexpression in the two remaining data sets (GSE7390 and GSE11121). After these filtering steps and after collapsing probes into unique genes, we had 681 genes for functional screening *in vitro*.

Each of the 681 genes was separately targeted with 4 different siRNA constructs. Hits were categorized by the number of constructs that inhibited cell growth, out of the maximum of 4 targeting any given gene. Twenty-seven genes had >2 siRNA hits (Supplementary Table 3) and two of these, LRP8 and VLDLR, had 3 hits.

Expression distribution of LRP8, VLDLR, APOE, Reelin, and DAB1 in breast cancer tissues, cell lines and normal tissues

Table 1 presents the mRNA expression distribution of LRP8, VLDLR, and its ligands APOE and reelin, as well as DAB1, a signal transducer intermediary of these receptors, in the 4 breast cancer tissue and 2 breast cancer cell line data sets. The co-expression of APOE and LRP8 and VLDLR were apparent in both the human cancer data sets and in cell lines. However, contrary to the expression in cancer tissues, in cell lines, we did not observe significant differential expression by ER-status. This raises the possibility that LRP8 is essential for *in vitro* survival and growth. Reelin and DAB expression were low in both the primary breast cancers and in cell lines. (Supplementary Figure 1) shows co-expression of these 5 molecules in 18 cell lines. Next we examined the mRNA expression of LRP8 and VLDLR in a broad range of normal tissues using the public MediSapiens website (www.medisapiens.com). In normal tissues, LRP8 was highly expressed in the testes, CNS, skin and placenta whereas VLDLR mRNA expression was more ubiquitous and was particularly high in the liver (Supplementary Figure 2). In the same database, we also assessed the expression of LRP8 in a broad range of different cancers. Subsets of B-cell acute lymphoid leukemia, glioma, lung, colorectal and ovarian cancers expressed high levels of LRP8, similar to TNBC (Supplementary Figure 3). These expression patterns suggest a better therapeutic window for LRP8, due to its limited expression in most normal tissues.

Validation of siRNA screen results and characterization of LRP8 and VLDLR effects *in vitro* and *in vivo*

We selected the BT-20, BT-549, MDA-MB-231, and MDA-MB-468 cell lines for further *in vitro* characterization of LRP8 and VLDLR effects. We confirmed the dose-dependent inhibitory effects of anti-LRP8 and anti-VLDLR siRNAs and the corresponding down regulation of the target mRNA and protein in all 4 cell lines (Figure 1a and Supplementary Figure 4). The pCMV-LRP8 and pCMV-VLDLR rescue vectors restored cell viability in all 4 cell lines exposed to siLRP8 or siVLDLR suggesting an LRP* and VLDLR mediated effect. (Figure 1b and Supplementary Figure 5).

Next, we examined the impact of knocking down shLRP8 in MDA-MB-231 cells injected into the mammary glands of nude mice. Significant reduction in tumor growth was observed by 3 weeks in

Table 1: Class comparison between ER+/Her2- and ER-/Her2- breast cancer.

LRP8 set								VLDLR set					
				ER+/Her2-		ER-/Her2-				ER+/Her2-		ER-/Her2-	
Data set	Number of samples	P value	FDR	Average	SD	Average	SD	P value	FDR	Average	SD	Average	SD
MDACC	133/65	<0.001	<0.001	296.8	181.0	558.4	227.4	<0.001	<0.001	252.8	176.8	491.8	258.0
Wang	178/56	<0.001	<0.001	137.9	108.0	296.8	130.4	<0.001	<0.001	250.5	129.6	460.1	277.1
TRANSBIG	124/46	<0.001	<0.001	215.6	126.8	421.9	271.0	<0.001	<0.001	236.1	129.1	389.6	205.1
Mainz	155/23	<0.001	<0.001	110.8	61.2	266.6	122.3	<0.001	<0.001	307.0	167.7	636.0	503.6
51 cell line	13/25	0.492	0.638	919.1	401.8	1060.9	784.1	0.135	0.422	439.0	218.4	680.2	1179.1
19 cell line	2/11	0.776	0.166	277.0	277.0	1145.0	688.2	0.386	0.815	339.1	16.7	469.2	322.5

RELN set								DAB set					
				ER+/Her2-		ER-/Her2-				ER+/Her2-		ER-/Her2-	
Data set	Number of samples	P value	FDR	Average	SD	Average	SD	P value	FDR	Average	SD	Average	SD
MDACC	133/65	0.130	0.163	109.9	100.5	133.9	282.7	0.936	0.936	32.0	39.6	31.7	33.0
Wang	178/56	0.678	0.689	160.7	125.5	153.9	355.6	0.689	0.689	21.2	16.3	20.4	22.7
TRANSBIG	124/46	0.224	0.280	83.4	152.9	68.2	87.8	0.051	0.084	14.6	15.3	11.9	9.1
Mainz	155/23	0.563	0.692	87.3	70.6	78.5	245.3	0.692	0.692	10.0	6.5	7.0	3.5
51 cell line	13/25	0.510	0.638	190.3	178.6	229.4	196.3	0.169	0.422	67.3	32.1	53.0	30.8
19 cell line	2/11	0.716	0.815	71.2	149.3	86.7	39.9	0.878	0.815	30.5	24.2	28.7	15.3

APOE set							
				ER+/Her2-		ER-/Her2-	
Data set	Number of samples	P value	FDR	Average	SD	Average	SD
MDACC	133/65	<0.001	<0.001	1549.0	1363.3	2160.3	2759.1
Wang	178/56	0.034	0.056	1943.8	1110.7	2278.7	2009.1
TRANSBIG	124/46	0.471	0.471	1609.0	711.1	1529.9	666.8
Mainz	155/23	<0.001	<0.001	1397.9	629.7	2037.0	1716.3
51 cell line	13/25	0.883	0.883	632.3	1236.2	654.1	1006.8
19 cell line	2/11	0.111	0.279	846.6	1337.9	384.7	226.0

ER: Estrogen Receptor, Her2: Human Epidermal Growth Factor Receptor 2. SD: Standard Deviation. P-value was based on normal distribution. P-values less than 0.05 were considered statistically significant.

Table 2: ApoE4 regulated proteins common to TNBC cell lines (BT-549 and MDA-MB-436).

ApoE4 upregulated proteins (n=5) Treated *vs* Control (T08)	**ApoE4 upregulated proteins (n=12) Treated *vs* Control (T48)**	
HIF1a p53 PKC-alpha_pS657 Snail VEGF	Caspase-7_cleavedD198 PTGS2 PTK2 HIF1a HistoneH2AX_pS139 MAP2K1	ERRFI1 CDKN1B MAPK14_pT180/182 p53 Rab25 Snail
ApoE4 downregulated proteins (n=1) Treated *vs* Control (T08)	**ApoE4 downregulated proteins (n=12) Treated *vs* Control (T48)**	
AMPK_pT172	AR Chk2_pT68 C-Raf_pS388 CyclinD1 EGFR EIF4EBP1_pS65/T70	HER2 RPS6_pS235/236/240/244 RPS6KB1 (p70S6K_pT389) SPARC Stat3_pY705 YAP

LRP8 knockdown cells compared to shRNA scrambled control or parental cells. This reduced growth persisted until the sacrifice of mice at 6 weeks after injection (Figure 2a). The percent of necrotic cells was significantly elevated in shLRP8 group compared to vector only control cells (17% *vs* 40%, p<0.01), whereas the fraction of mitotic cells were similar in both cohorts (Figure 2b).

Stimulation of LRP8 or VLDLR with ApoE increase cell growth in an isoform dependent manner

The 4 cell lines were treated with reelin and three distinct human ApoE isoforms; ApoE2, ApoE3, and ApoE4. These isoforms differ in 2 amino acids and have distinct receptor binding affinities. Reelin caused a modest, but significant 0.8 to 1-fold increase in cell growth in a dose- and time-dependent manner (Supplementary Figure 6). ApoE2 showed a slight inhibitory effect, ApoE3 had no measurable effect, whereas ApoE4 demonstrated a dramatic stimulatory effect with 2-6 fold increase in cell growth by the end of the 72-hour exposure period (Figure 3a).

Next, we examined if ApoE4 effected cell proliferation and apoptosis as measured by BrdU uptake and caspase 3/7 activation, respectively. ApoE4 significantly increased BrdU incorporation in a dose-dependent manner, but caspase activity was not altered (Figure 3b). siRNA knockdown of LRP8 abolished the proliferative effects of ApoE4 but also significantly increased apoptosis (Supplementary Figure 7). To test if ApoE induced proliferation is mediated through LRP8, we exposed cells simultaneously to ApoE4 and RAP1 which inhibits binding of ApoE to lipoprotein receptors. The addition of RAP1 abolished the stimulatory effect of ApoE4 in all 4 cell lines (Figure 3c).

ApoE4 treatment stimulates proliferation and survival of TNBC cells during serum starvation in a LRP8-mediated manner

ApoE4 treatment rescued TNBC cells from serum-starvation induced growth arrest and this effect required LRP8 expression. To

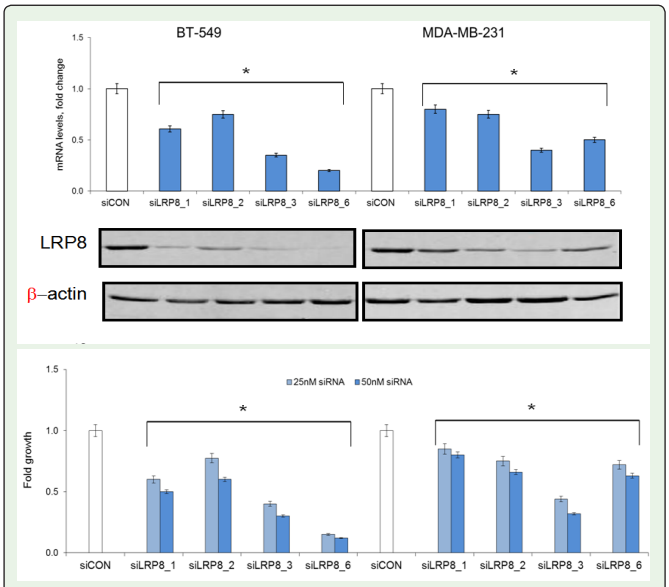

Figure 1A: Identification of LRP8 and VLDLR as potential target genes for triple-negative breast cancer.
a) mRNA and protein down-regulation was observed after siLRP8 transfection, with concurrent growth inhibition after 25 and 50 nM siLRP8. LRP8 mRNA and protein levels are shown for 50 nM of siLRP8. Representative data from replicate experiments in four TNBC cell lines, BT-20, BT-549, MDA-MB-231, and MDA-MB-436 (* indicate p<0.05).

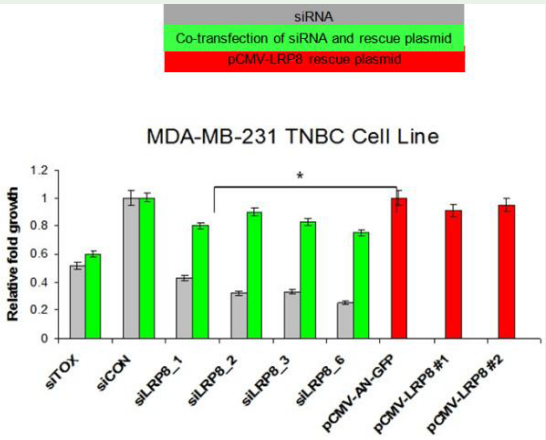

Figure 1B: Plasmid rescue validation experiments confirmed that growth inhibition was due to siRNA-mediated down regulation of LRP8. MDA-MB-231 cells were transfected with siLRP8 alone, LRP8 rescue plasmid with silent mutations in the siRNA binding region, or the combination of siLRP8 and rescue plasmid. TNBC cell viability was rescued with the combination of siLRP8 and rescue plasmid. Representative data from replicate experiments in four TNBC cell lines, BT-20, BT-549, MDA-MB-231, and MDA-MB-436 (*indicate p<0.05).

Table 3: LRP8 protein expression and its relation to clinicopathologic variables of breast cancer patients.

Clinicopathologic variables		Number	LRP8 positive*	LRP8 negative*	p-value***
All cases		49	n (%)	n (%)	
			44 (90)	5 (10)	
Age	<50	19	17 (39)	2 (40)	1
	≥50	30	27 (61)	3 (60)	
ER	positive	25	23 (52)	2 (40)	1
	negative	23	21 (48)	2 (40)	
	unknown	1	0	1 (20)	
HER2**	positive	13	13 (30)	0	0.5627
	negative	35	31 (70)	4 (80)	
	unknown	1	0	1 (20)	
Stage	I	3	2 (5)	1 (20)	0.2343
	II-III	45	42 (95)	3 (60)	
	unknown	1	0	1 (20)	
T	T0-T1	32	29 (66)	3 (60)	1
	T2-3	16	15 (34)	1 (20)	
	unknown	1	0	1 (20)	
N	NX-N1	41	36 (82)	5 (100)	0.5751
	N2-N3	8	8 (18)	0	
Nuclear grade	I-II	14	13 (30)	1 (20)	1
	III-IV	34	31 (70)	3 (60)	
	unknown	1	0	1 (20)	
Ki67	High expression	24	23 (52)	1 (20)	0.025
	Low expression	3	1 (3)	2 (40)	
	unknown	22	20 (45)	2 (40)	

*LRP8 positive was considered strong and moderate immunostaining on IHC. LRP8 negative was considered weak immunostaining.
**HER2 positive was considered >2+ score on IHC. Ki67 high expression was considered >10% immunostaining.
***p-values are based on Fisher's exact test with n ≤5. Two-sided, 95% confidence interval, α<0.05.

study the mechanism of this effect we performed gene expression profiling of BT-549 and MDA-MB-436 with and without ApoE4 exposure under serum-free conditions, controls also included cells grown in regular media. Serum starvation induced extensive gene expression changes by 8 hours with further changes by 48 hours (Supplementary Table 4-5). Many of these changes were cell line specific, but 108 and 67 genes showed consistent up- and down-regulation in both cell lines at 48 hours (Supplementary Table 6). Most of the shared up-regulated genes were enzymes involved in steroid biosynthesis, and lipid and amino acid metabolism pathways. Down-regulated genes were involved with mitosis and nucleotide metabolism (Supplementary Figure 8a). The lipid biosynthesis network connecting the starvation-induced genes centered on the transcription factor SREBF2 (Supplementary Figure 8c). ApoE4 treatment mitigated or altogether reversed these starvation induced gene expression changes in cells grown in serum-free media (Supplementary Figure 8b and 8d).

Reverse phase protein array analysis of the same two cell lines under similar conditions (serum-free and regular media, with and without ApoE4 stimulation) also identified 24 and 20 consistently up and down-regulated proteins in both cell lines by 48hours (Supplementary Table7). The up-regulated and/or activated proteins were interconnected through the MAPK signaling network (Supplementary Figure 9a, Table 2). Proteins which were down-regulated after ApoE4 treatment were involved in ribosomal assembly and protein translation (Supplementary Figure 9b, Table 2).

To confirm the array findings and to assess if these effects of ApoE4 are mediated by the LRP8 receptor, we performed Western blotting of select proteins in LRP8 knockdown BT-549 cells and the MDA-MB-231 cells used in the Xenograft model (Supplementary Figure 9c). LRP8 knockdown efficiency was similar in both cell lines. We confirmed that COX2, SNAIL, RAB25 expression as well as Phosphorylation of H2AX (pS139) increased after ApoE exposure and these responses were abolished or abrogated in cells treated with siLRP8 indicating a receptor mediated effect. In MDA-MB-231 cells, these responses were detectable but less pronounced.

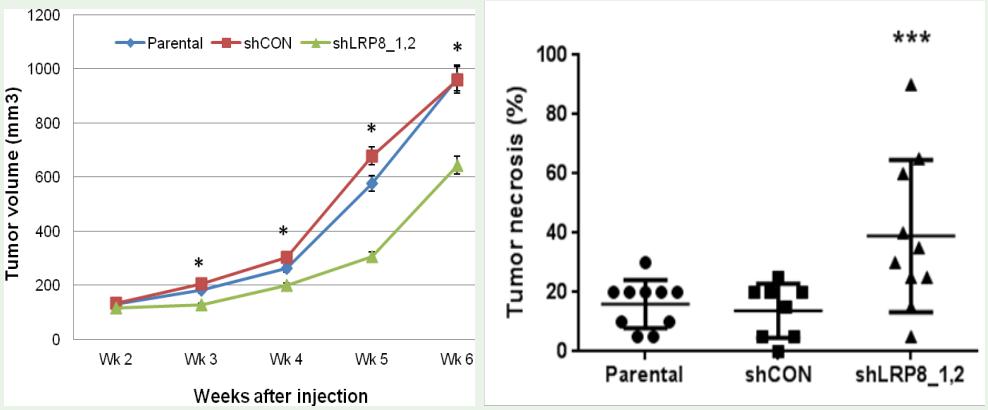

Figure 2: LRP8 contributes to xenograft growth *in vivo*.
a) MDA-MB-231 parental, shCON, and shLRP8 Xenograft were established in 4 week old nude mice (n=12 per group). The mean of tumor volumes of each group were tested with one-way ANOVA analysis (* indicate p<0.05).
b) Tumor sections were examined for the presence of tumor necrosis as a percentage of total tumor section per slide and compared with mitotic cells per slide were counted. The mean tumor necrosis of each group were tested with one-way ANOVA analysis (* indicate p<0.01).

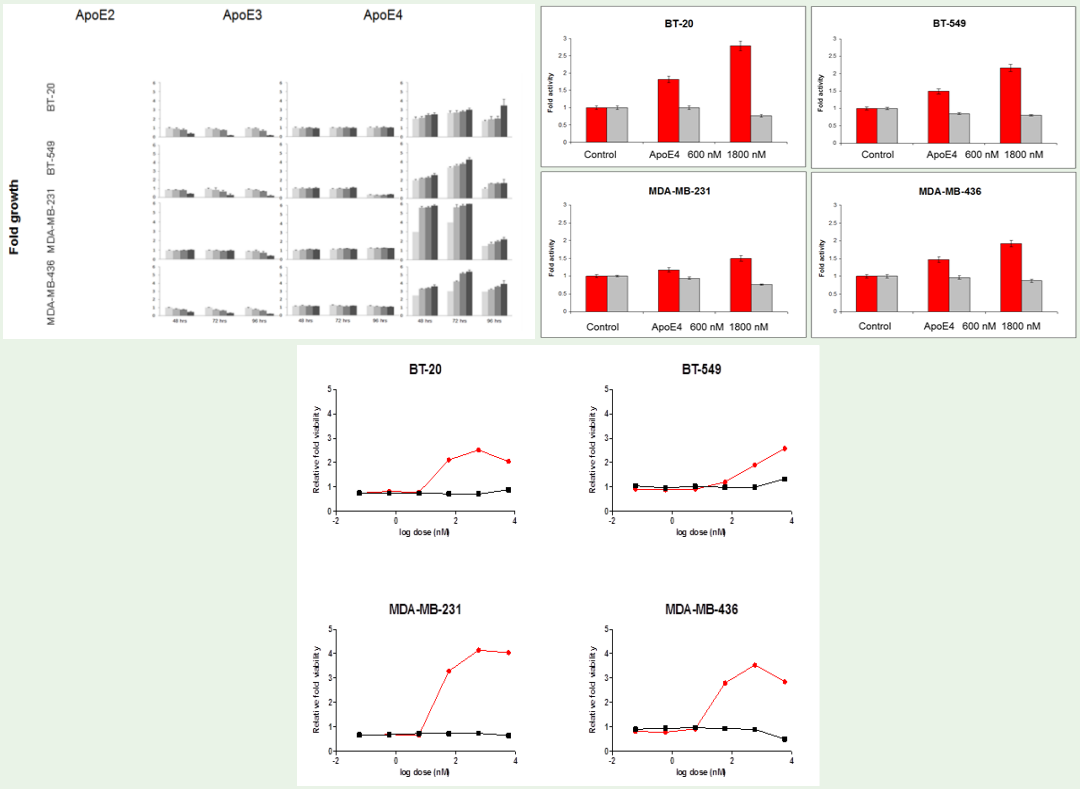

Figure 3: LRP8/VLDLR - APOE receptor - ligand signaling system.
a) ApoE isoform 2 inhibited TNBC cell growths in a dose-dependent manner, ApoE isoform 3 did not affect growth, and ApoE isoform 4 promoted growth of TNBC cell lines. The proliferative effect was dose-dependent in ApoE2 and ApoE4 from 150 to 1200 nM of ApoE, with reduced proliferation after 72 hours of treatment.
b) ApoE4 increased BrdU incorporation (shown in red) after 48 hours of treatment, increasing in activity from 600 to 1200nM of ApoE4. Caspase 3, 7 activities did not significantly change.
c) RAP treatment (black lines) abolished the ApoE4 stimulatory effect (red lines) when 200nM of RAP was combined with greater than 150nM of ApoE4 after 48 hours of treatment.

Metabolomic profiling of cells under serum starvation exposed to ApoE4

Parental and LRP8 knockdown BT-549 cells were treated with ApoE4 and metabolic profiling was performed at 48 hours, controls included cells grown in regular media and in serum free media without ApoE4. The growth of cells in serum-free media compared with regular media induced significant changes in 147 of 273 measured metabolites at 48 hours (Supplementary Table 8). The changes induced by serum starvation suggested increased oxidative stress and decreased proliferation. This data set also showed that exposure to ApoE4 during serum starvation decreased these metabolic changes including alterations in glycolysis intermediates and PPP-associated metabolites (ribose and xylitol). ApoE4 also reversed effects of serum starvation on the TCA cycle intermediate succinate and fatty acids and arachidonate.

Again, these metabolic effects of ApoE4 were dependent on the expression of LRP8 and could be abrogated by LRP8 siRNA. Nucleic acid metabolites, inosine, guanosine and uridine, were more abundant in cells with SF media relative to regular media, and knocking LRP8 down further increased the levels of these nucleosides, while exposure to ApoE4 had the opposite effect. Levels of 3'AMP (a degradation product of 2'3'-cAMP) were also affected in opposing directions by LRP8 knockdown and ApoE4 addition. Intermediates to nucleotide synthesis that are components of the pentose phosphate pathway (ribose-5-phosphate and the ribulose-5-phosphate isobar) also had similar patterns. ApoE4 exposure increased the levels of 7α-hydroxycholesterol and 7β-hydroxycholesterol and the cholesterol precursor lanosterol, which occurred in the absence of any serum or lipid supplementation.

LRP8 Immunohistochemistry

Of the 59 human breasts cancer samples 49 yielded results (5 slides had no tumor cells for assessment, in 1 case the tissue floated, and 4 cases with conflicting accession numbers between the slide label and IHC reading. Thirteen tumors showed strong, 11 moderate, and 20 weak staining; 5 cases were completely negative. There was a trend for stronger LRP8 expression in high nuclear grade cancers and high Ki67 expression was significantly associated with positive LRP8 staining (p=0.025). (Table 3)

Discussion

We identified 681 genes that were consistently and significantly overexpressed in TNBC in multiple data sets and performed a siRNA screen including each of these genes on 18 breast cancer cell lines. Two closely related cell surface receptors, LRP8 and VLDLR showed

the most consistent inhibitory effect in our siRNA screen and were therefore selected for further mechanistic studies *in vitro* and *in vivo*. Both of these receptors mediate cholesterol and lipid trafficking through binding to Apoliporotein E (ApoE) in peripheral tissues and function as stress signaling pathways through binding reelin in neural cells in the central nervous system [14]. In the brain, binding of these ligands to LRP8/VLDLR leads to src family kinase-mediated phosphorylation of the adapter protein DAB1 which subsequently activates the Phosphatidylinositol 3-Phopshate Kinase (PI3K) and AKT and Glycogen Synthase Kinase (GSK3b) pathways [15]. To our knowledge, our study is the first to identify the function of LRP8 - ApoE4 receptor system in the growth of TNBC. We demonstrate that LRP8 and VLDLR are critical survival factors for TNBC cells, particularly under starvation and enable cells to maintain metabolic activity. These events do not appear to be mediated via DAB1. Down regulation of either LRP8 or VLDLR, or blocking of ApoE binding to these receptors, results in increased apoptosis *in vitro* and *in vivo*. Cells treated with ApoE4 undergo major metabolic changes when grown under serum free conditions. ApoE4 treatment reverses (or delays the development of many of the metabolic effects of serum starvation.

Based on these experiments, we hypothesize that LRP8 is not just a passive trans-membrane transporter of lipids but also initiates signaling events when activated by its ligand ApoE that increase lipid metabolism and other metabolic events that are required for cell growth. Its high expression in cell lines suggest that this receptor and its signaling function is important for *in vitro* survival of cells. It is noteworthy that TNBC which also have high expression of LRP8 tend to also have high metabolic activity which is readily detectable by PET-CT. The relatively low expression of LRP8 in most normal tissues coupled with its high expression in TNBC and its essential function for cell survival under nutrient stress renders it a potential novel therapeutic target for this disease.

References

1. Liedtke C, Mazouni C, Hess KR, Andre F, Tordai A, Mejia JA, et al. Response to neoadjuvant therapy and long-term survival in patients with triple-negative breast cancer. J Clin Oncol. 2008; 26: 1275-1281.
2. Gluz O, Liedtke C, Gottschalk N, Pusztai L, Nitz U, Harbeck N. Triple-negative breast cancer: Current status and future directions. Ann Oncol. 2009; 20: 1913-1927.
3. Rouzier R, Perou CM, Symmans WF, Ibrahim N, Cristofanilli M, Anderson K, et al. Breast cancer molecular subtypes respond differently to preoperative chemotherapy. Clin Cancer Res. 2005; 11: 5678-5685.
4. Jiang Y, Harlocker SL, Molesh DA, Dillon DC, Stolk JA, Houghton RL, et al. Discovery of differentially expressed genes in human breast cancer using subtracted cDNA libraries and cDNA microarrays. Oncogene. 2002; 21: 2270-2282.
5. Pusztai L, Ayers M, Stec J, Clark E, Hess K, Stivers D, et al. Gene expression profiles obtained from fine-needle aspirations of breast cancer reliably identify routine prognostic markers and reveal large-scale molecular differences between estrogen-negative and estrogen-positive tumors. Clin Cancer Res. 2003; 9: 2406-2415.
6. Sotiriou C, Neo SY, McShane LM, Edward LK, Philip ML, Amir Jazaeri, et al. Breast cancer classification and prognosis based on gene expression profiles from a population-based study. Proc Natl Acad Sci USA. 2003; 100: 10393-10398.
7. Sotiriou C, Pusztai L. Gene-expression signatures in breast cancer. N Engl J Med. 2009; 360: 790-800.
8. Perou CM, Sorlie T, Eisen MB, van de Rijn M, Jeffrey SS, Rees CA, et al. Molecular portraits of human breast tumours. Nature. 2000; 406: 747-752.
9. Sorlie T, Perou CM, Tibshirani R, Aas T, Geisler S, Johnsen H, et al. Gene expression patterns of breast carcinomas distinguishes tumor subclasses with clinical implications. Proc Natl Acad Sci USA. 2001; 98: 10869-10874.
10. The Cancer Genome Atlas Network. Comprehensive molecular portraits of human breast tumours. Nature 2012; 490: 61-70.
11. Arnedos M, Bachelot T, Campone M, De La Cruz , Commo F, Mathieu MC, et al. Array CGH and PIK3CA/AKT1 mutations to drive patients to specific targeted agents: A clinical experience in 108 patients with metastatic breast cancer. Eur J Cancer. 2012; 48: 2293-2299.
12. Shiang C, Qi Y, Wang B, Lazar V, Wang J, Fraser Symmans W, et al. Amplification of fibroblast growth factor receptor-1 in breast cancer and the effects of brivanib alaninate. Breast Cancer Res Treat. 2010; 123: 747-755.
13. Stratowa C, Wilgenbus KK. Gene expression profiling in drug discovery and development. Current Opinion in Molecular Therapeutics. 1999; 1: 671-679.
14. Nimpf J, Schneider WJ. From cholesterol transport to signal transduction: low density lipoprotein receptor, very low density lipoprotein receptor, and apolipoprotein E receptor-2. Biochim Biophys Acta. 2000; 1529: 287-298.
15. Yang XV, Banerjee Y, Fernandez J, Hiroshi Deguchi, Xiao Xu, Laurent O. Mosnier, et al. Activated protein C ligation of ApoER2 (LRP8) causes Dab1-dependent signaling in U937 cells. Proc Natl Acad Sci USA. 2009; 106: 274-279.
16. MAQC Consortium, Shi L, Reid LH, Jones WD, Shippy R, Warrington JA, et al. The MicroArray Quality Control (MAQC) project shows inter- and intraplatform reproducibility of gene expression measurements. Nature Biotech. 2006; 24: 1151-1161.
17. Wang Y, Klijn JG, Zhang Y, Sieuwerts AM, Look MP, Yang F, et al. Gene-expression profiles to predict distant metastasis of lymph-node-negative primary breast cancer. Lancet. 2005; 365: 671-679.
18. Gong Y, Yan K, Lin F, Anderson K, Sotiriou C, Andre F, et al. Determination of oestrogen-receptor status and ERBB2 status of breast carcinoma: A gene-expression profiling study. Lancet Oncol. 2007; 8: 203-211.
19. Pounds S, Morris SW. Estimating the occurrence of false positive and false negatives in microarray studies by approximating and partitioning the empirical distribution of p-values. Bioinformatics. 2003; 19: 1236-1242.
20. Desmedt C, Piette F, Loi S, Wang Y, Lallemand F, Haibe-Kains B, et al. Strong time dependence of the 76-gene prognostic signature for node-negative breast cancer patients in the TRANSBIG multicenter independent validation series. Clin Cancer Res. 2007; 13: 3207-3214.
21. Schmidt M, Bohm D, von Torne C, Steiner E, Puhl A, Pilch H, et al. The humoral immune system has a key prognostic impact in node-negative breast cancer. Cancer Res. 2008; 68: 5405-5413.
22. Neve RM, Chin K, Fridlyand J, Yeh J, Baehner FL, Fevr T, et al. A collection of breast cancer cell lines for the study of functionally distinct cancer subtypes. Cancer Cell. 2006; 10: 515-527.
23. Liedtke C, Wang J, Tordai A, Symmans WF, Hortobagyi GN, Kiesel L, et al. Clinical evaluation of chemotherapy response predictors developed from breast cancer cell lines. Breast Cancer Res Treat. 2010; 121: 301-309.
24. Tibes R, Qiu Y, Lu Y, Hennessy B, Andreeff M, Mills GB, et al. Reverse phase protein array: Validation of a novel proteomic technology and utility for analysis of primary leukemia specimens and hematopoietic stem cells. Mol Cancer Ther. 2006; 5: 2512-2521.
25. Dehaven CD, Evans AM, Dai H. Organization of GC/MS and LC/MS metabolomics data into chemical libraries. J Cheminform. 2010; 2: 1-12.